Climate and marine carbon cycle response to changes in the strength of the Southern Hemispheric westerlies

L. Menviel,[1] A. Timmermann,[2] A. Mouchet,[3] and O. Timm[2]

Received 1 February 2008; revised 2 June 2008; accepted 19 June 2008; published 4 October 2008.

[1] It has been previously suggested that changes in the strength and position of the Southern Hemisphere westerlies could be a key contributor to glacial-interglacial atmospheric CO_2 variations. To test this hypothesis, we perform a series of sensitivity experiments using an Earth system model of intermediate complexity. A strengthening of the climatological mean surface winds over the Southern Ocean induces stronger upwelling and increases the formation of Antarctic Bottom Water. Enhanced Ekman pumping brings more dissolved inorganic carbon (DIC)-rich waters to the surface. However, the stronger upwelling also supplies more nutrients to the surface, thereby enhancing marine export production in the Southern Hemisphere and decreasing the DIC content in the euphotic zone. The net response is a small atmospheric CO_2 increase ($\sim$5 ppmv) compared to the full glacial-interglacial CO_2 amplitude of $\sim$90 ppmv. Roughly the opposite results are obtained for a weakening of the Southern Hemisphere westerly winds.

Citation: Menviel, L., A. Timmermann, A. Mouchet, and O. Timm (2008), Climate and marine carbon cycle response to changes in the strength of the Southern Hemispheric westerlies, *Paleoceanography*, *23*, PA4201, doi:10.1029/2008PA001604.

1. Introduction

[2] Atmospheric CO_2 concentrations recorded in ice cores [*Petit et al.*, 1999] covaried with temperature and ice volume changes on orbital time scales. While glacial-interglacial CO_2 changes of 80–90 ppmv certainly affected global climate via the greenhouse effect, the origin of these CO_2 variations still remain elusive. Colder and drier climate conditions during glacial times were associated with a reduced terrestrial carbon stock. Hence, to account for the glacial CO_2 drop, large amounts of carbon must have been sequestered in the ocean. Different mechanisms have been suggested such as increased CO_2 solubility, greater Southern Ocean stratification and sea ice cover [*Francois et al.*, 1997; *Stephens and Keeling*, 2000; *Gildor et al.*, 2002], deepening of the lysocline [*Archer et al.*, 2000] and increased marine export production due to either greater marine nutrient inventory [*Broecker*, 1982, 1998; *McElroy*, 1983], or a higher Redfield ratio [*Broecker*, 1982; *Omta et al.*, 2006], or an increase in iron availability in surface waters [*Martin*, 1990]. So far, however, model results and theoretical considerations [*Archer et al.*, 2003] suggest that there does not seem to be a single mechanism that can explain the full magnitude of the glacial-interglacial atmospheric CO_2 changes as well as their timing.

[3] Recently, *Toggweiler et al.* [2006] (hereinafter referred to as T06) proposed that an overall weakening of the Southern Hemispheric westerlies during glacial times could have led to a substantial drawdown of atmospheric CO_2. The reasoning proposed in T06 is the following: Presently, strong Southern Hemispheric westerlies generate a northward Ekman transport that leads to upwelling of nutrient and CO_2-rich waters. A potential equatorward shift or weakening of the westerlies during glacial periods could have substantially reduced the supply of carbon-rich deep waters to the surface, leading to an enhanced uptake of carbon in the Southern Ocean. An atmospheric CO_2 reduction leads to global cooling, and presumably an extension of the Southern Hemispheric sea ice belt around Antarctica. Not only could this substantially reduce the air-sea fluxes of CO_2 [*Stephens and Keeling*, 2000], but also move the westerlies farther equatorward. T06 estimated that this positive feedback could explain an atmospheric CO_2 reduction of about 35 ppmv. It should however be noted that the model employed in T06 does neither capture sea ice dynamics properly, nor does it consider a primary production consistent with the modified circulation. Indeed the primary production in T06 is evaluated after restoring the surface phosphate content to the present-day observed values. Firstly, we will show that paleoproxy data as well as the PMIP2 coupled model simulations are at odds with the notion of a significant equatorward shift of the Southern Hemispheric westerlies. Secondly, our study will demonstrate that variable phosphate concentrations would alter the T06 result substantially.

[4] As approximately 40% of the anthropogenic CO_2 sequestration in the oceans occurs in the Southern Ocean [*Sabine et al.*, 2004; *Mikaloff Fletcher et al.*, 2006], understanding the impacts of Southern Hemispheric wind changes on this CO_2 sink at present and for future projections is of great importance. Some recent modeling studies suggest

[1] Department of Oceanography, University of Hawai'i, Honolulu, Hawaii, USA.
[2] IPRC, SOEST, University of Hawai'i, Honolulu, Hawaii, USA.
[3] Département AGO, Université de Liège, Liège, Belgium.

0883-8305/08/2008PA001604$12.00

that the strengthening and poleward shift of the Southern Hemispheric westerlies observed over the last 30 years [*Thompson and Solomon*, 2002] may have weakened the CO_2 sink in the Southern Ocean [*LeQuéré et al.*, 2007; *Lovenduski et al.*, 2007]. However, these results have been recently challenged by *Law et al.* [2008] and *Zickfeld et al.* [2008].

[5] Our study is organized as follows: The intermediate model setup for the wind sensitivity experiments is described in section 2. In section 3 several paleoproxy records that are sensitive to Southern Hemispheric westerly winds will be discussed. The section also reviews the glacial wind response in a series of coupled model simulations for the Last Glacial Maximum (LGM, 21 ka B.P.). The results from the wind sensitivity experiments will then be described in section 4. The T06 hypothesis will be tested for enhanced and reduced westerlies as well as for a fully prognostic phosphate concentration and a climatologically prescribed one. The paper concludes with a summary of our main results and a discussion.

2. Model and Experimental Setup

[6] The model used in this study is the Earth system model of intermediate complexity, LOVECLIM [*Menviel et al.*, 2008], which is based on a somewhat simplified atmosphere model, an ocean general circulation model, a dynamic-thermodynamic sea ice model, and oceanic as well as terrestrial carbon cycle components. For the sake of simplicity, the model experiments presented here employ a stationary preindustrial vegetation pattern.

[7] The atmospheric component of the coupled model LOVECLIM is ECBilt [*Opsteegh et al.*, 1998], a spectral T21, three-level model, based on quasi-geostrophic equations extended by estimates of the neglected ageostrophic terms [*Lim et al.*, 1991]. The model contains a full hydrological cycle which is closed over land by a bucket model for soil moisture. Synoptic variability associated with weather patterns is explicitly simulated. Diabatic heating due to radiative fluxes, the release of latent heat and the exchange of sensible heat with the surface are parameterized. Compared to the standard version of LOVECLIM we enhanced the sensitivity of ECBilt to longwave radiation forcing by a factor of 2 [*Timm and Timmermann*, 2007]. The simulated global mean temperature response to such a CO_2 doubling amounts to about 3°C as compared to the standard sensitivity of 1.5°C.

[8] The ocean-sea ice component of LOVECLIM, CLIO [*Goosse et al.*, 1999; *Goosse and Fichefet*, 1999; *Campin and Goosse*, 1999] consists of a free-surface primitive equation ocean model with $3° \times 3°$ resolution coupled to a thermodynamic-dynamic sea ice model. Coupling between atmosphere and ocean is done via the exchange of freshwater and heat fluxes. To avoid a singularity at the North Pole, the oceanic component makes use of two subgrids: The first one is based on classic longitude and latitude coordinates and covers the whole ocean except for the North Atlantic and Arctic Ocean. These are covered by the second spherical subgrid, which is rotated and has its poles at the equator in the Pacific (111°W) and Indian Ocean (69°E).

[9] LOCH is a three-dimensional global model of the oceanic carbon cycle with prognostic equations for dissolved inorganic carbon (DIC), total alkalinity, phosphates (PO_4^{3-}), organic products, oxygen and silicates [*Mouchet and Francois*, 1996; *Fichefet et al.*, 2007; *Menviel et al.*, 2008]. LOCH is fully coupled to CLIO, using the same time step as CLIO. In addition to their biogeochemical transformations, tracers in LOCH are advected with the CLIO circulation field and experience horizontal and vertical mixing. The near-surface oceanic uptake of CO_2 is governed by the solubility as well as the regional biological processes. The partial pressure of CO_2 in the surface waters is calculated from the total alkalinity and DIC tracers. The difference between the partial pressure of CO_2 in the ocean and in the atmosphere, modulated by a wind-dependent exchange coefficient, determines the net CO_2 air-sea fluxes. LOCH computes the export production from the state of a phytoplankton pool in the euphotic zone (0–120 m). The phytoplankton growth depends on the availability of nutrients (PO_4^{3-}) and light, with a weak temperature dependence. A grazing process together with natural mortality limit the primary producer's biomass and provide the source term for the organic matter sinking to depth. Remineralization of organic matter depends on oxygen availability, but anoxic remineralization can also occur. Depending on the silicate availability, phytoplankton growth is accompanied by the formation of opal or $CaCO_3$ (calcite and aragonite) shells, which then sink to depth. $CaCO_3$ shells are dissolved depending on the calcite and aragonite saturation states, whereas a simple constant rate is used for opal. The organic matter that is not remineralized and the shells that are not dissolved are permanently preserved in the sediments. This leads to a loss of alkalinity, carbon, phosphates and silicates, which is compensated for by the river influx of these components. The atmospheric CO_2 content is predicted for each ocean time step from the air-sea CO_2 fluxes calculated by LOCH.

[10] The preindustrial steady state (PIN) was obtained by forcing LOVECLIM with 278 ppmv of atmospheric CO_2 during 500 years, then allowing the atmospheric CO_2 to vary freely during 700 years. The model was then run for 500 years with fixed preindustrial vegetation. All sensitivity experiments described in this paper start from this initial state.

[11] In experiment WINDP (WINDM), the zonal and meridional 10 m wind velocities between 60 and 40°S were increased (decreased) by about 15%. The wind modifications were applied in the atmosphere-ocean-sea-ice coupling routine. Not only is the wind stress forcing of the ocean modified but also the latent and sensible heat fluxes, in contrast to the model setup of T06. To better understand the effects of changes of marine primary production on the atmospheric CO_2, we also repeated WINDM using a climatologically prescribed phosphate field, WINDMCP. WINDP, WINDM and WINDMCP were run for 1,000 years.

3. Paleoproxies and Modeling Studies of the Southern Hemisphere Westerlies During the LGM

[12] Several recent pollen studies from Chile suggest a wetter climate west of the Andes during the LGM than at present [*Moreno et al.*, 1999; *Maldonado et al.*, 2005; *Valero-Garcés et al.*, 2005]. Corroborating evidence comes

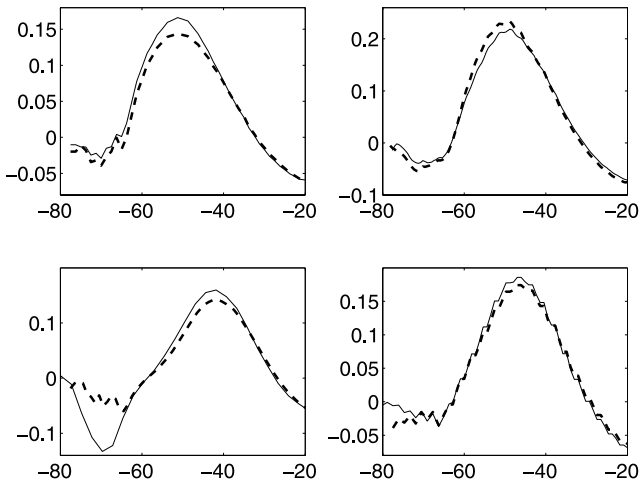

Figure 1. Zonally averaged zonal wind stress component (Pa) corresponding to the preindustrial (solid line) and LGM (dashed line) simulations for the models (top left) HadCM3M2, (top right) CCSM3, (bottom left) IPSL, and (bottom right) MIROC-medres.

also from marine sediments cores from the Chilean margin [*Lamy et al.*, 1999; *Stuut and Lamy*, 2004]. The possible mechanism to explain the greater precipitation is an equatorward shift and/or an intensification of the Southern Hemisphere westerly winds and of the storm track [*Garreaud*, 2007]. However, these recent studies are in disagreement with other paleostudies: Reconstructed drier LGM conditions in southern America [*Markgraf et al.*, 1992] have been explained in terms of weaker westerlies and a weaker storm track. Trying to reconcile these conflicting paleodata, *Shulmeister et al.* [2004] analysis indicates that Southern Hemispheric westerlies were stronger during the LGM than for interglacial conditions.

[13] Ice cores from the Antarctic Peninsula suggest that the flux of dust originating from Patagonia was much larger during the LGM than at present [*Basile et al.*, 1997; *Petit et al.*, 1999; *Delmonte et al.*, 2002]. The main mechanisms which can explain the enhanced dust flux are (1) increased westerly winds and (2) drier conditions in the source region, which would be compatible with the hypothesis of weaker westerly storm tracks. Therefore, dust records from Antarctic ice cores do not provide unambiguous information on the strength of the Southern Hemisphere westerlies.

[14] It is fair to say that the existing paleoproxy data do not allow for a very accurate reconstruction, neither of the strength, nor of the position of the mean glacial Southern Hemispheric westerlies.

[15] To test the conjecture of shifted or reduced glacial westerlies (T06) we analyze preindustrial and LGM Coupled General Circulation Model (CGCM) simulations that were compiled as part of the Paleoclimate Modeling Intercomparison Project (PMIP2). All PMIP2 LGM CGCMs employ the same forcing: the ICE-5G ice sheet reconstruction for the period 21 ka B.P. [*Peltier*, 2004], prescribed glacial greenhouse gas concentrations, lowered sea level and insolation anomalies due to variations in the Earth's orbit [*Braconnot et al.*, 2007].

[16] Our analysis focuses on the preindustrial and LGM simulations that were conducted using a fixed continental vegetation cover [*Braconnot et al.*, 2007]. We analyze the results from four PMIP2 CGCMs: the HadCM model (the UK Met Office HadCM3M2 model [*Gordon et al.*, 2000]), the CCSM3 model (National Center for Atmospheric Research CCSM3 model [*Otto-Bliesner et al.*, 2006]), the IPSL model (Institut Pierre Simon Laplace, IPSL-CM4-V1-MR model [*Marti et al.*, 2005]) and the MIROC model (CCSR/NIES/FRCGC/MIROC3.2.2 medres model [*K-1 Model Developers*, 2004]). The simulated wind changes in these models are also compared with the ones obtained for our LOVECLIM LGM simulation [*Menviel et al.*, 2008]. The latter differs somewhat from the PMIP protocol: we use the ICE-4G orographic reconstruction, a fully interactive vegetation model and the present-day sea level.

[17] Figure 1 shows the zonal component of the annual wind stress zonally averaged for the preindustrial (solid line) and LGM (dashed line) simulations for the HadCM3M2, CCSM3, IPSL-CM4-V1 and MIROC3.2 CGCMs. The HadCM3M2 and the IPSL model exhibit weaker Southern Hemispheric westerlies (−12%) during the LGM, whereas the CCSM3 simulates stronger westerlies (+8%) in both hemispheres. The Southern Hemispheric wind stress anomalies in the MIROC model are relatively small (−6%). Consistent with the CCSM3 model result, LOVECLIM also simulates stronger westerlies under LGM conditions (not shown). Most strikingly however, none of the CGCMs simulates large meridional shifts of the westerlies in the Southern Ocean, in contrast to the T06 conjecture of equatorward shifted westerlies under glacial conditions. Even for the same boundary conditions, the strength of the zonally averaged annual mean glacial Southern Hemispheric westerlies differs considerably among the CGCMs. Analyzing the PMIP2 LGM CGCMs simulations, *Rojas et al.* [2008] find a more consistent pattern of weakened wintertime westerlies in the South Pacific region.

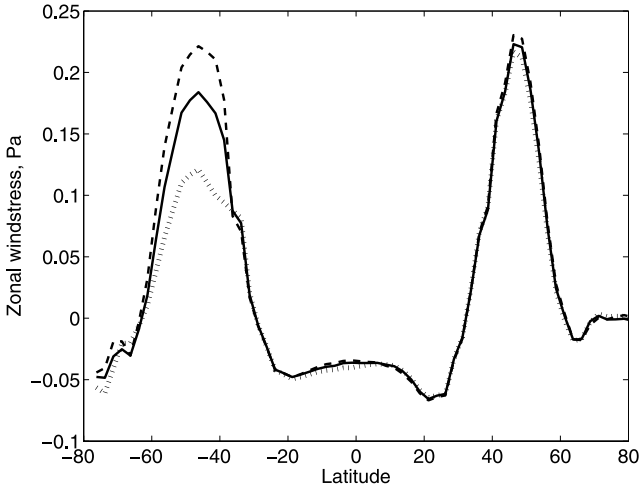

Figure 2. Zonal wind stress component (Pa) zonally averaged for PIN (solid line), WINDP (dashed line), and WINDM (dotted line). The last 50 years of PIN were averaged as well as the modeling years 480−500 of WINDP and WINDM.

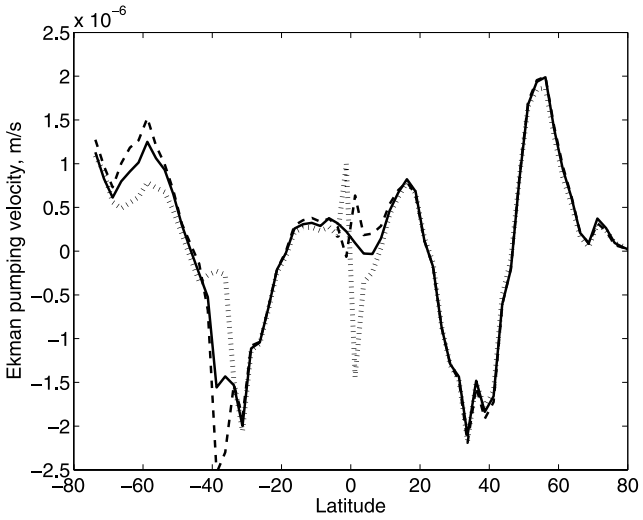

Figure 3. Same as Figure 2 but for Ekman pumping velocity zonally averaged (m/s) for PIN (solid line), WINDP (dashed line), and WINDM (dotted line).

[18] In summary, neither the proxy data nor the CGCM simulations make a strong case for equatorward shifted or substantially weakened zonal mean westerlies during the LGM, in contrast to the T06 hypothesis.

4. Results

4.1. Climate

[19] The forced increase in Southern Hemispheric 10 m winds in experiment WINDP leads to a 22% greater zonal wind stress in this area (Figure 2). As a result, the Antarctic Circumpolar Current (ACC) strengthens and the mass transport through Drake passage increases by about 40%. The northward anomalous Ekman transport enhances upwelling of Circumpolar Deep Water (CDW) (Figures 3 and 4). Because the upwelled deep water is colder and saltier than the surface waters an overall cooling (Figure 3) and salinity increase (not shown) are observed near the surface. The stronger 10 m winds also lead to increased evaporation (+20%), which further cools the ocean surface and increases surface salinity south of 40°S. On the other hand, the greater northward Ekman transport in the Southern Ocean induces more convergence around 40°S and therefore increased

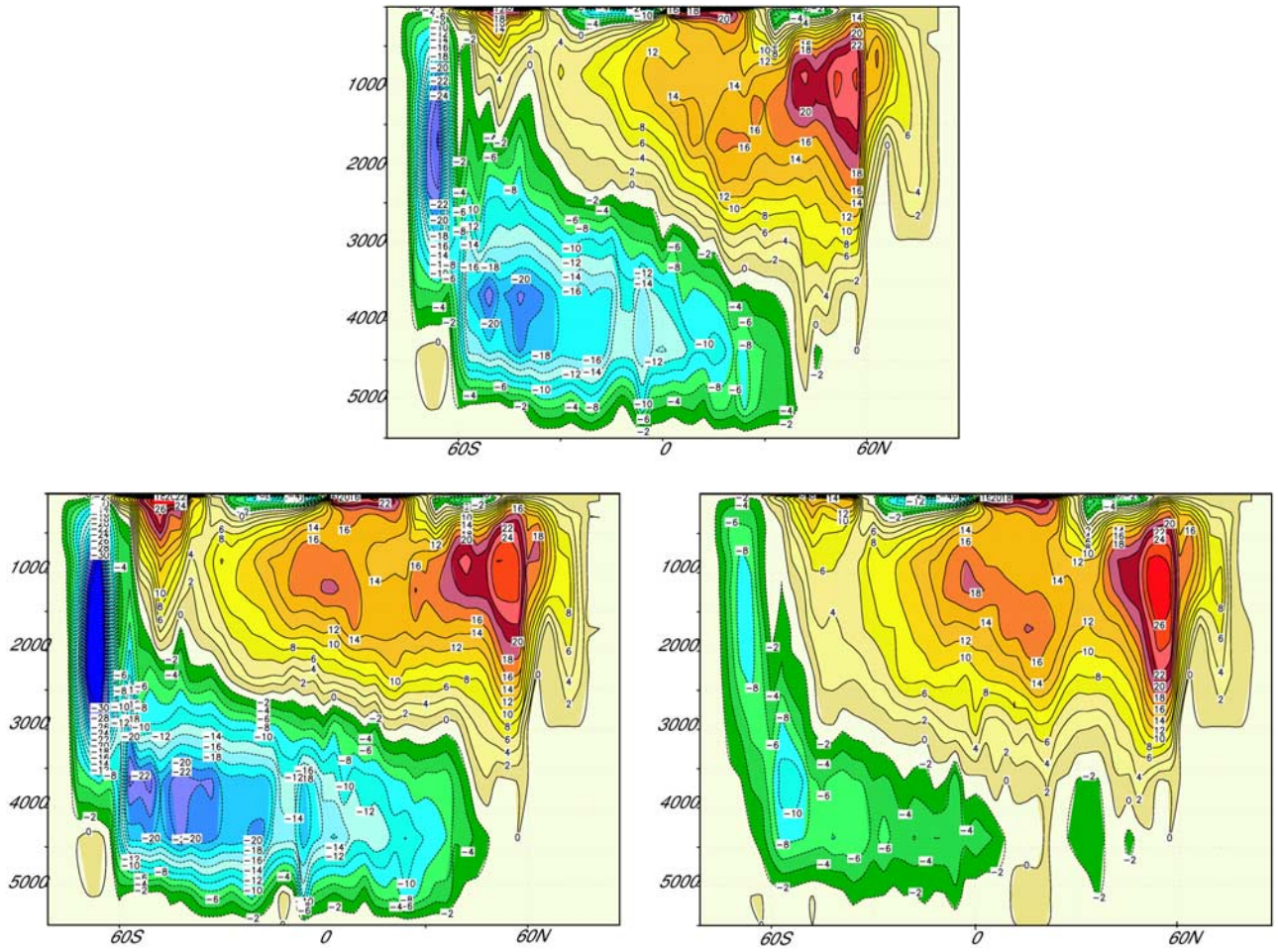

Figure 4. Global stream function (Sv) (top) averaged for the last 50 years of the control run (PIN) and averaged for years 450–500 of experiments (bottom left) WINDP and (bottom right) WINDM.

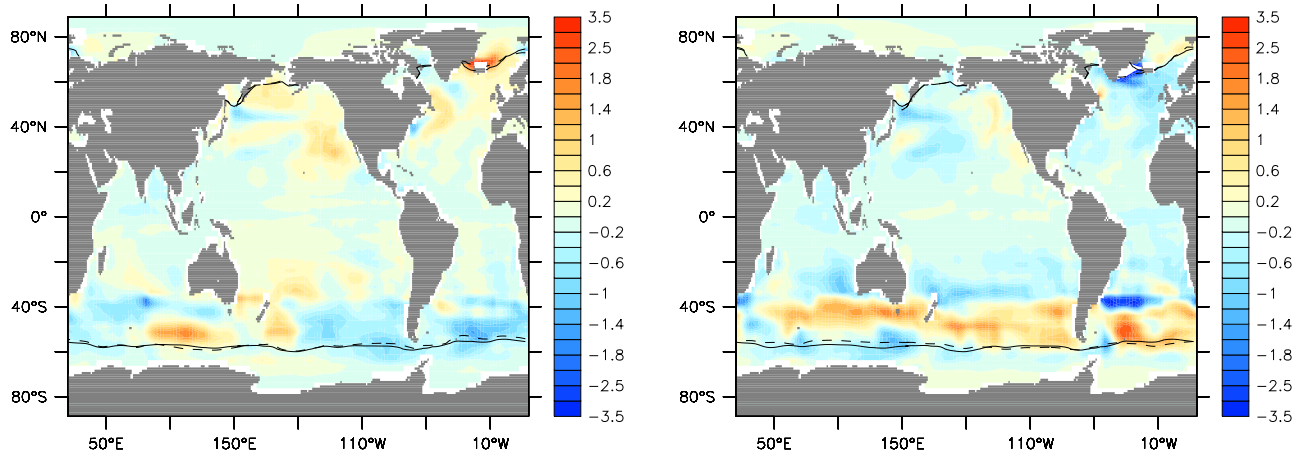

Figure 5. SST anomalies (°C) for (left) WINDP-PIN and (right) WINDM-PIN. The solid line represents the sea ice thickness contour at 0.1 m for PIN, and the dashed line displays the sea ice thickness contour at 0.1 m averaged for the years 600–1000 for WINDP (Figure 5, left) and WINDM (Figure 5, right).

downwelling there (Figure 3). In the WINDP simulation we obtain an increase in the production of AABW from 16 Sv to 32 Sv. This can be partly explained by the increased surface density. This increase of AABW is likely to affect also the overall strength of the ACC by processes described by *Cai and Baines* [1996].

[20] As a result of stronger upwelling and evaporation, the Southern Ocean cools initially in the latitudinal band of 40–60°S. However, after about 40 years, a positive SST anomaly develops between 100–150°E that can be related to ocean circulation anomalies. Understanding the mechanism of these advective anomalies is beyond the scope of the paper. A possible mechanism might involve a wind-induced spin-up of the Southern Hemispheric supergyre [*Cai*, 2006]. Furthermore, as a result of stronger AABW formation and the increased equatorward export of cold water in the bottom layers, an increased poleward heat transport (not shown) occurs that balances the surface heat loss during convection near Antarctica. While the surface density south of 40°S increases, the slope of the isopycnals steepens near the surface leading to an enhanced heat transport via larger bolus velocities [*Gent and McWilliams*, 1990]. This effect has been described in detail by *Stocker et al.* [2007].

[21] The reduction in 10 m winds over the Southern Ocean in WINDM and WINDMCP leads to a 33% decrease of the zonally averaged zonal wind stress component (Figure 2). Because of reduced Ekman pumping near Antarctica (Figure 3) the upwelling of CDW decreases. Reduced Ekman pumping increase the SST between 40°S and 60°S by up to 2.5°C (Figure 5). The weaker winds also lead to a 20% decrease in evaporation over the Southern Ocean, which induces a freshening of the surface waters and a reduction of the latent heat flux. The resulting net decrease of surface density leads to a reduction of AABW production from 16 Sv to 10 Sv (−38%) (Figure 4). In addition, the poleward heat transport decreases by about 40%. Reduced zonal winds and reduced AABW formation eventually lead to a weakening of the ACC transport through Drake Passage by about 30%.

[22] As will be discussed below, the WINDMCP experiment that mimics the abiotic response to weakened westerlies, simulates a significantly lower CO_2 concentration than the WINDM experiment. This leads to an additional global cooling and a reduced warming between 40°S and 60°S compared to WINDM.

4.2. Marine Biochemical Response

[23] As can be seen in Figure 6, anomalously strong upwelling in experiment WINDP causes an increase in the euphotic phosphate (PO_4^{3-}) content (+9%) south of 30°S. The marine export production therefore increases by 7% in the latitudinal band 30–60°S.

[24] For experiment WINDM, weaker Southern Ocean upwelling of phosphates into the euphotic zone (∼−20%) lead to a 14% reduction in export production between 30–60°S (Figure 6).

[25] Under present-day conditions a part of the upwelled waters in the Southern Ocean is exported northward through Ekman transport and is partly incorporated into the Subantarctic Mode Water (SAMW). At low latitudes, this water mixes into the thermocline and can eventually be upwelled in the major upwelling zones [*Marinov et al.*, 2006]. The nutrient excess in WINDP or the deficit in WINDM can therefore be transmitted to the low latitudes. As can be seen on Figure 6, the phosphate content is greater in the euphotic zone from the Southern Ocean to the northern tropics in WINDP, and lower in WINDM. However, for experiment WINDP, there is a negative anomaly in the euphotic phosphate content in the eastern equatorial Pacific, which could be the result of a deepening of the thermocline and of the nutricline. The globally averaged phosphate concentration in the euphotic zone is significantly larger in the WINDP experiment than in the WINDM experiment. Hence the global export production increases by +4% in WINDP, whereas it decreases by 10% for WINDM. This has important consequences for the CO_2 fluxes in these two experiments, as will be discussed below.

[26] In the control experiment, DIC-enriched waters are upwelled to the surface in the Southern Ocean enhancing

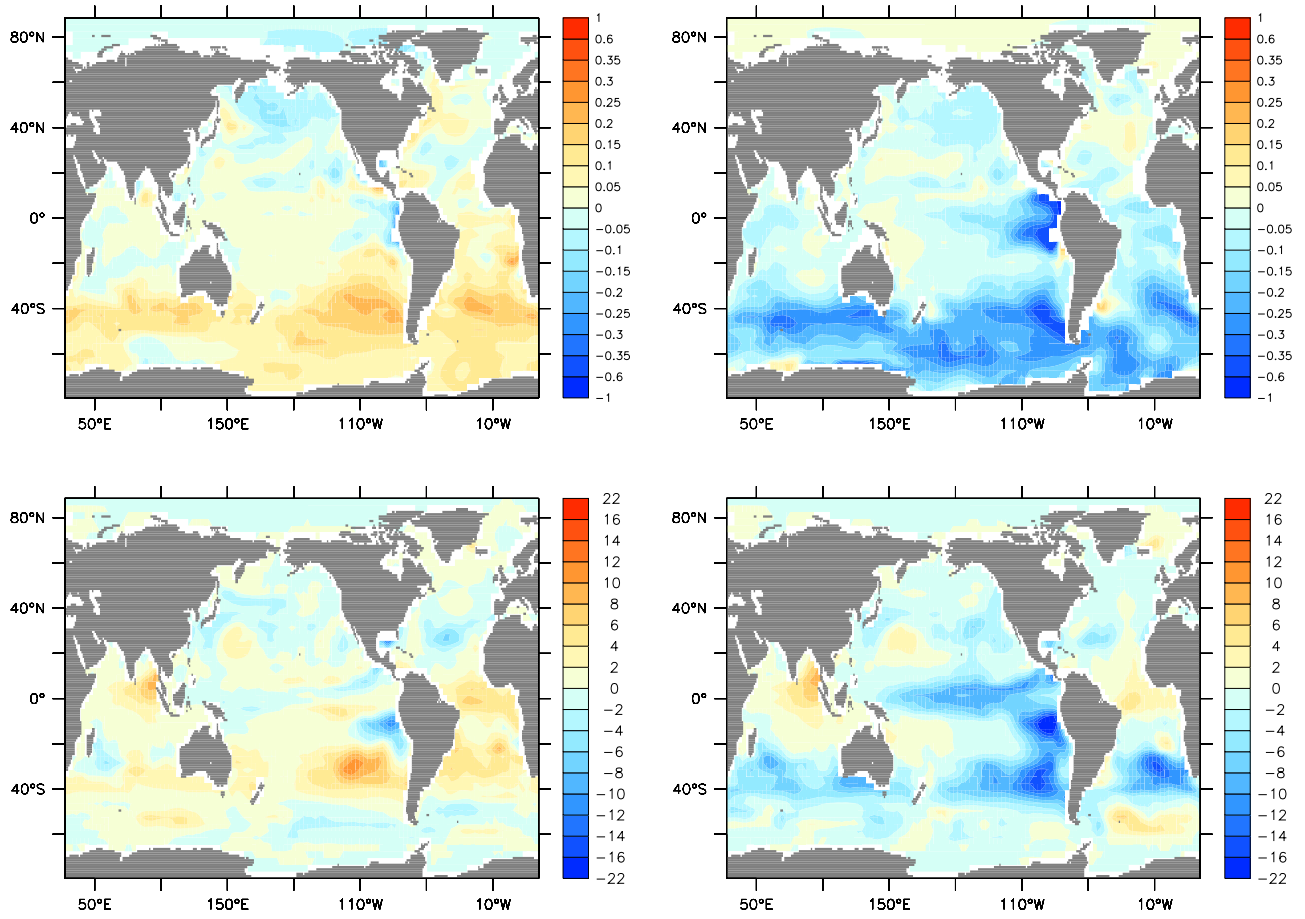

Figure 6. (top) Phosphate anomalies (μmol/l) averaged over the euphotic zone for the years 600–1000 for (left) WINDP-PIN and (right) WINDM-PIN. (bottom) Same as Figure 6 (top) but for export production (gC/m^2/a).

the partial pressure of CO_2 in the ocean and reducing the net flux of CO_2 from the atmosphere to the ocean. In experiment WINDP, the stronger Southern Hemispheric westerlies enhance the upwelling of DIC-rich waters as documented in Figure 7. Compared to the control run, the thermocline waters south of 20°N contains about 25 μmol/l more DIC, which leads to a substantial increase in mean oceanic carbon release in the latitudinal band 35–50°S. On the other hand, south of 50°S, even with the greater amount of DIC-rich waters brought to the surface, the ocean still acts as a sink of carbon. Negative temperature anomalies compensate for the DIC increase in surface waters. Stronger winds result in a sink that is even larger in that area in experiment WINDP as compared to PIN (Figure 8).

[27] In the WINDM experiment weaker westerlies reduce the outcropping of DIC-rich waters (Figure 7). Compared to the control run, the surface waters south of 20°N in WINDM have about 40 μmol/L less DIC, whereas the DIC accumulates in the deeper parts of the ocean. This dramatic DIC decrease in the upper layers of the Southern Ocean more than compensates the warming in that area. As a result, south of 30°S the ocean acts now as a net sink of CO_2 (Figure 8). The change is clearly visible around 40°S where the net source during PIN reverses into a weak sink during WINDM.

[28] For the final quasi-equilibrium stages of WINDP the oceanic carbon stock has lost about 8 GtC, which induces a net atmospheric CO_2 increase of about 4 ppmv (Figure 9). For WINDM, the oceanic carbon stock increases by about 10 GtC, which induces a net atmospheric CO_2 decrease of about 5 ppmv. This is much smaller than simulated by T06. In contrast to T06, however, our export production is varying because of the enhanced/weakened upwelling of nutrient-rich waters. In fact, for both sensitivity experiments, WINDP and WINDM, the simulated changes in export production have the tendency to compensate the DIC effect on Southern Hemispheric CO_2 fluxes.

[29] To better quantify the effects of anomalous export production on the atmospheric CO_2, we performed an experiment in which the three-dimensional PO_4^{3-} field is kept at its climatological value, as diagnosed from the preindustrial control run. Therefore, the export production is basically the same as in PIN. Only minor differences in marine export production may occur as a consequence of temperature variations. The relative change in global export production with respect to PIN amounts to about 1%. As can be seen in Figure 7, the larger export production in

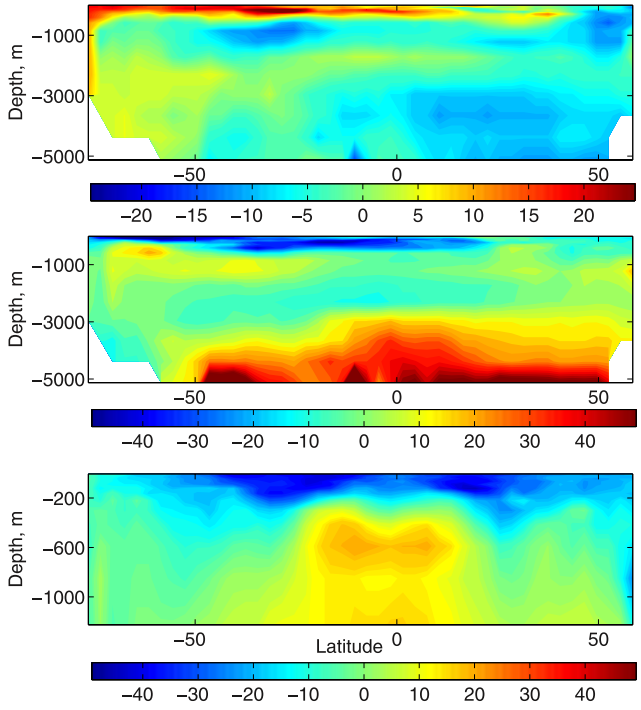

Figure 7. DIC anomaly (μmol/l) in the Pacific basin (latitude versus depth) for (top) WINDP-PIN, (middle) WINDM-PIN, and (bottom) WINDMCP-WINDM. Please note that the color scale of Figure 7 (top) is different from the color scale of Figure 7 (middle and bottom).

WINDMCP compared to WINDM leads to a DIC deficit at the surface of the Pacific Ocean that is 40 μmol/L greater in WINDMCP than in WINDM. This supports the notion that the lower export production in WINDM compensates for a large part the changes in DIC content brought about by the varying upwelling. In the Southern Ocean (between 40°S and 60°S), the changes in DIC, alkalinity, SST and SSS lead to a local pCO_2 decrease of 32 ppmv, which is twice more than that simulated by WINDM. The local pCO_2 in WINDMCP in the latitudinal band 20–40°S is about 20 ppmv lower than in the control experiment, whereas it is only 4 ppmv lower in WINDM. After 1000 simulation years, the ocean carbon stock in WINDMCP has gained about 35 GtC, which leads to a net atmospheric CO_2 decrease of 18 ppmv (Figure 9). The results of WINDMCP are more comparable to the T06 solution. However, in reality the export production is very likely to vary with the wind variations, thereby damping the CO_2 effect of wind-induced DIC anomalies substantially.

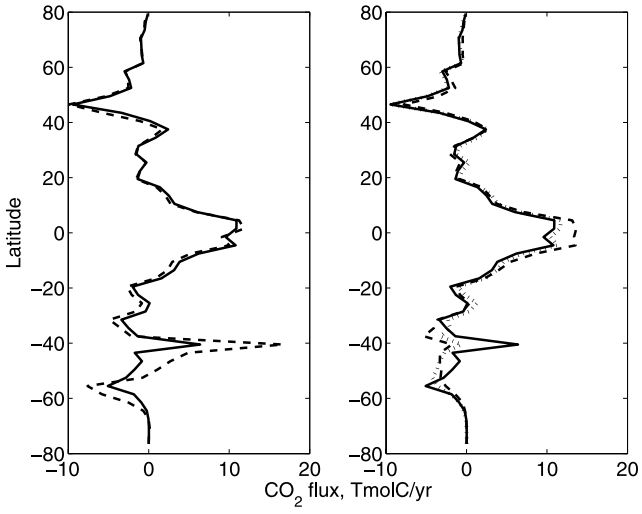

Figure 8. Zonally averaged flux of CO_2 (TmolC/a) from the ocean to the atmosphere averaged for the last 400 years of runs (left) PIN (solid line) and WINDP (dashed line) as well as (right) PIN (solid line), WINDM (dotted line), and WINDMCP (dashed line). Please note that a negative value indicates an ocean sink.

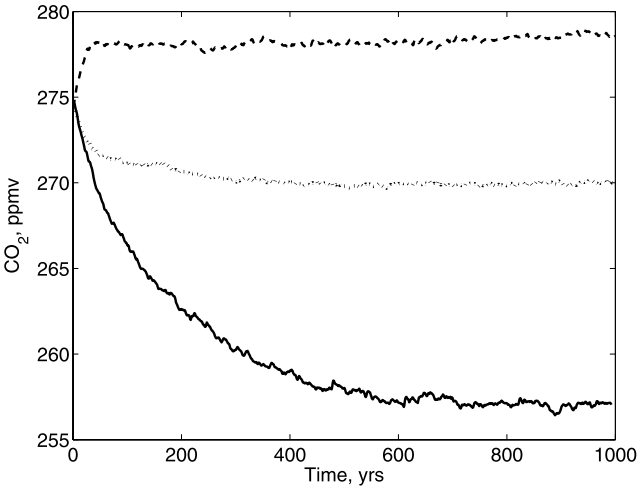

Figure 9. Atmospheric CO_2 time series (ppmv) for WINDP (dashed line), WINDM (dotted line), and WINDMCP (solid line).

4.3. Summary and Discussion

[30] T06 suggested that changes in the strength and position of the Southern Hemispheric westerlies could have an important impact on glacial-interglacial atmospheric CO_2 variations. To test this hypothesis we performed a series of experiments using an Earth system model of intermediate complexity fully coupled to a marine carbon cycle model. Weaker westerlies in these simulations lead to decreased Ekman pumping near Antarctica. The upwelling of CDW is therefore reduced by about 40%, which causes a reduction in the amount of DIC-rich as well as nutrient rich cold waters brought to the surface. As the partial pressure of CO_2 (pCO_2w) is a function of the DIC concentration in the surface water, the reduced upwelling therefore induces a lower pCO_2w. Carried by the SAMW, nutrient anomalies are transported all the way up to 10°N in the Pacific. The resulting globally averaged negative export production anomaly therefore counteracts the effect of DIC changes on atmospheric CO_2. The net effect is a drop of atmospheric CO_2 by 5 ppmv. The crucial role of export production was further highlighted in the wind sensitivity experiment with the fixed phosphate, WINDMCP. Indeed when surface DIC

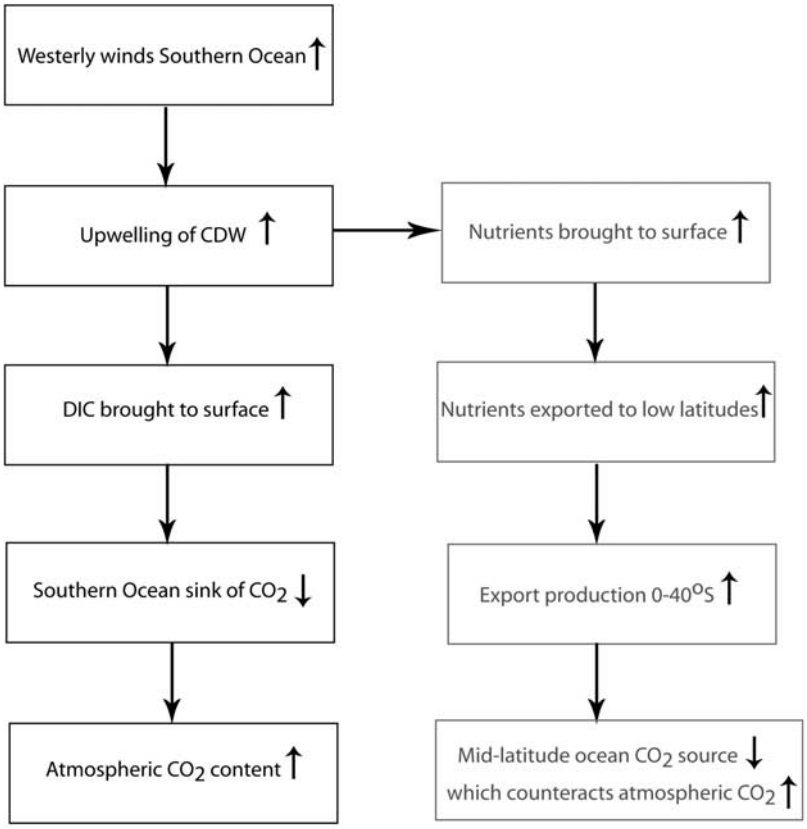

Figure 10. (left) A concise representation of T06's hypothesis and (right) the additional role of export production in counteracting the atmospheric CO_2 increase presented in this paper.

content is only influenced by changes in oceanic transport and solubility, the atmospheric CO_2 decreases by 18 ppmv. For an increase in surface wind strength by 15%, roughly the opposite results are obtained.

[31] When increasing the Southern Ocean wind stress, T06 obtained oscillations between a state with an active AABW formation and a state without any AABW formation. Using constant enhanced wind forcing, the associated variations in atmospheric CO_2 attained magnitudes of up to 35 ppmv. The two different oceanic circulation regimes of T06 are quite similar to the ones obtained in our WINDP and WINDM experiments. However, our 5 ppmv atmospheric CO_2 response contrasts with the T06 result. The wind sensitivity experiment with the fixed phosphate (WINDMCP) demonstrated that this difference can be explained by the compensating effect of export production anomalies, mainly in between 30°S and 50°S, that were neglected in T06. While our modeling results clearly document the importance of changes in export production for the glacial wind sensitivity, it should be noted that neglecting that contribution, as in T06, we are able to reproduce the main results described in T06. Figure 10 concisely summarizes T06's hypothesis as well as the counteracting effect due to changes in export production described in this paper.

[32] In our modeling study, the dependence of primary production on iron as well as vegetation changes were not taken into account. In the Southern Hemisphere, the strength of the westerlies correlates well with the strength of the storm track. In fact transient eddy activity in the storm track plays a key role in organizing the Southern Annual Mode [*Jin et al.*, 2006] as well as the mean westerlies. Weaker storms and weaker mean westerlies are likely to result in less Australian and Patagonian dust deposition in the Southern Ocean and hence a reduced iron fertilization. This may result in reduced export production in the Southern Ocean, thereby amplifying the phosphate effect described here. On the other hand, extended source areas and a drier atmosphere could be factors that enhance the dust deposition. To complete our analysis, we also performed a similar experiment to WINDP but with an interactive vegetation and terrestrial carbon component (VECODE module). The globally colder and drier conditions lead to a small release of carbon from the vegetation. The ocean buffers this release, which induces a net atmospheric CO_2 increase of only 4 ppmv. Hence the vegetation effects do not alter our main conclusions.

[33] The results presented here are in agreement with the study performed by *Winguth et al.* [1999], using the carbon cycle HAMOCC3 coupled online with the Hamburg Large Scale geostrophic ocean general circulation model (LSG OGCM). For a 10% enhancement of the Southern Hemisphere westerlies, they obtained an atmospheric CO_2 increase of only 2 ppmv while the global export production increases by 10%. Our results are also supported and complemented by a recent modeling study using a 3D ocean model fully coupled

to a marine carbon cycle model [*Tschumi et al.*, 2008]. In response to variations in the Southern Hemisphere westerlies of ±50%, *Tschumi et al.* [2008] obtain ±10 ppmv changes in atmospheric CO_2, when their model is tuned to a realistic strength of the meridional overturning circulation. However, in their study, the nutrient anomalies generated in the Southern Ocean are not transported to low latitudes.

[34] On the basis of the fact that neither paleoproxies, nor the PMIP LGM simulations provide strong support for weaker Southern Hemispheric westerlies, we conclude that the scenario described in T06 is a very uncertain scenario. Moreover, our model results suggest that weaker or equatorward shifted westerlies would lead to only marginal CO_2 variations due to the compensating effects of reduced DIC and nutrient upwelling. We therefore suggest that wind changes in the Southern Ocean are an unlikely candidate to explain a large fraction of the glacial-interglacial CO_2 variations. Further modeling studies using coupled models would be needed to investigate the uncertainties associated with our results.

[35] This study is also relevant to understand the importance of recent changes in the Southern Hemispheric westerlies on the sequestration of anthropogenic CO_2. It has been observed that, since the 1970s, the winds over the Southern Ocean have shifted poleward and intensified [*Thompson and Solomon*, 2002] presumably because of ozone depletion in the stratosphere [*Sexton*, 2001]. Our study demonstrates a rather complex air-sea CO_2 flux response to intensifying winds (Figure 8): stronger upwelling of DIC rich waters induces a greater outgassing of CO_2 near 40°S, whereas the CO_2 sink centered at 60°S is enhanced because of the stronger winds and colder conditions. In addition, north of 35°S, a simulated increased export production leads to an enhanced sequestration of CO_2. In agreement with earlier studies [*Lenton and Matear*, 2007; *LeQuéré et al.*, 2007; *Lovenduski et al.*, 2007], a strengthening of the Southern Hemispheric westerlies induces a slight weakening of the CO_2 sink in the Southern Ocean. However, for intensifying winds and sustained anthropogenic CO_2 emissions, the greater level of atmospheric CO_2 might overcompensate the effect of the wind-induced upwelling of DIC as already argued by *Zickfeld et al.* [2008]. Our results also reveal the importance of middle- and low-latitude export production changes in partly offsetting the effects of high-latitude changes in surface DIC.

[36] **Acknowledgments.** This research was supported by NSF grant ATM06-28393. Additional support was provided by the Japan Agency for Marine-Earth Science and Technology (JAMSTEC), by NASA through grant NNX07AG53G, and by NOAA though grant NA17RJ1230 through their sponsorship of research activities at the International Pacific Research Center. A. Mouchet acknowledges support from the Belgian Science Policy (BELSPO contract SD/CS/01A). We are grateful to Richard Zeebe for his encouragement to pursue this study. We thank the anonymous reviewers for their helpful comments. We acknowledge the international modeling groups for providing their data for analysis and the Laboratoire des Sciences du Climat et de l'Environnement (LSCE) for collecting and archiving the model data. The PMIP2/MOTIF Data Archive is supported by CEA, CNRS, the EU project MOTIF (EVK2-CT-2002-00153), and the Programme National d'Etude de la Dynamique du Climat (PNEDC). The analyses were performed using version 11-01-2007 of the database. More information is available at http://pmip2.lsce.ipsl.fr/ and http://motif.lsce.ipsl.fr/. This is IPRC publication 526 and SOEST contribution 7472.

References

Archer, D., A. Winguth, D. W. Lea, and N. Mahowald (2000), What caused the glacial/interglacial atmospheric pCO_2 cycles?, *Rev. Geophys.*, *38*, 159–189.

Archer, D. E., P. A. Martin, J. Milovich, V. Brovkin, G. Plattner, and C. Ashendel (2003), Model sensitivity in the effect of Antarctic sea ice and stratification on atmospheric pCO_2, *Paleoceanography*, *18*(1), 1012, doi:10.1029/2002PA000760.

Basile, I., F. E. Grousset, M. Revel, J.-R. Petit, P. E. Biscaye, and N. I. Barkov (1997), Patagonian origin of glacial dust deposited in East Antarctica (Vostok and Dome C) during glacial stages 2, 4 and 6, *Earth Planet. Sci. Lett.*, *146*, 573–579.

Braconnot, P., et al. (2007), Results of PMIP2 coupled simulations of the Mid-Holocene and Last Glacial Maximum—Part 1: Experiments and large-scale features, *Clim. Past*, *3*, 261–277.

Broecker, W. S. (1982), Ocean chemistry during glacial time, *Geochim. Cosmochim. Acta*, *46*, 1689–1705.

Broecker, W. S. (1998), Paleocean circulation during the last deglaciation: A bipolar seesaw?, *Paleoceanography*, *13*, 119–121.

Cai, W. (2006), Antarctic ozone depletion causes an intensification of the Southern Ocean supergyre circulation, *Geophys. Res. Lett.*, *33*, L03712, doi:10.1029/2005GL024911.

Cai, W., and P. G. Baines (1996), Interactions between thermohaline- and wind-driven circulations and their relevance to the dynamics of the Antarctic Circumpolar Current in a coarse-resolution global ocean general circulation model, *J. Geophys. Res.*, *101*, 14,073–14,093.

Campin, J. M., and H. Goosse (1999), Parameterization of density-driven downsloping flow for a coarse-resolution ocean model in z-coordinate, *Tellus, Ser. A*, *51*, 412–430.

Delmonte, B., J. R. Petit, and V. Maggi (2002), Glacial to Holocene implications of the new 27000-year dust record from the EPICA Dome C (East Antarctica) ice core, *Clim. Dyn.*, *18*, 647–660.

Fichefet, T., E. Driesschaert, H. Goosse, P. Huybrechts, I. Janssens, A. Mouchet, and G. Munhoven (2007), Modelling the evolution of climate and sea level during the third millennium (MILMO), *Proj. EV/09*, Belg. Sci. Policy, Brussels. (Available at http://www.belspo.be/belspo/home/publ/pub\ostc/EV/rappEV09\en.pdf)

Francois, R., M. A. Altabet, E. F. Yu, D. M. Sigman, M. P. Bacon, M. Frank, G. Bohrmann, G. Bareille, and L. D. Labeyrie (1997), Contribution of Southern Ocean surface-water stratification to low atmospheric CO_2 concentrations during the last glacial period, *Nature*, *389*, 929–935.

Garreaud, R. (2007), Precipitation and circulation covariability in the extratropics, *J. Clim.*, *20*, 4789–4797.

Gent, P. R., and J. C. McWilliams (1990), Isopycnal mixing in ocean circulation models, *J. Phys. Oceanogr.*, *20*, 150–155.

Gildor, H., E. Tziperman, and J. R. Toggweiler (2002), Sea ice switch mechanism and glacial-interglacial CO_2 variations, *Global Biogeochem. Cycles*, *16*(3), 1032, doi:10.1029/2001GB001446.

Goosse, H., and T. Fichefet (1999), Importance of ice-ocean interactions for the global ocean circulation: A model study, *J. Geophys. Res.*, *104*(C10), 23,337–23,355.

Goosse, H., E. Deleersnijder, T. Fichefet, and M. H. England (1999), Sensitivity of a global coupled ocean-sea ice model to the parameterization of vertical mixing, *J. Geophys. Res.*, *104*(C6), 13,681–13,695.

Gordon, C., C. Cooper, C. A. Senior, H. Banks, J. M. Gregory, T. C. Johns, J. F. B. Mitchell, and R. A. Wood (2000), The simulation of SST, sea-ice extents and ocean heat transports in a version of the Hadley Center Model without flux adjustments, *Clim. Dyn.*, *16*, 147–168.

Jin, F.-F., L.-L. Pan, and M. Watanabe (2006), Dynamics of synoptic eddy and low-frequency flow interaction. Part I: A linear closure, *J. Atmos. Sci.*, *63*, 1677–1694.

K-1 Model Developers (2004), K-1 Coupled GCM (Miroc description) 1, edited by H.|Hasumi and S.|Emori, *Tech. Rep. 1*, Cent. for Clim. Syst. Res., Univ. of Tokyo, Tokyo. (Available at http://

www.ccsr.u-tokyo.ac.jp/kyosei/hasumi/MIROC/tech-repo.pdf)

Lamy, F., D. Hebbeln, and G. Wefer (1999), High-resolution marine record of climatic change in mid-latitude Chile during the last 28,000 years based on terrigenous sediment parameters, *Quat. Res.*, *51*, 83–93.

Law, R. M., R. J. Matear, and R. J. Francey (2008), Comment on "Saturation of the Southern Ocean CO_2 sink due to recent climate change", *Science*, *319*, 570.

Lenton, A., and R. J. Matear (2007), Role of the Southern Annular Mode (SAM) in Southern Ocean CO_2 uptake, *Global Biogeochem. Cycles*, *21*, GB2016, doi:10.1029/2006GB002714.

LeQuéré, C., et al. (2007), Saturation of the Southern Ocean CO_2 sink due to recent climate change, *Science*, *316*, 1735–1738.

Lim, G. H., J. R. Holton, and J. M. Wallace (1991), The structure of the ageostrophic wind field in baroclinic waves, *J. Atmos. Sci.*, *48*, 1733–1745.

Lovenduski, N. S., N. Gruber, S. C. Doney, and I. D. Lima (2007), Enhanced CO_2 outgassing in the Southern Ocean from a positive phase of the Southern Annular Mode, *Global Biogeochem. Cycles*, *21*, GB2026, doi:10.1029/2006GB002900.

Maldonado, A., J. L. Betancourt, C. Latorre, and C. Villagran (2005), Pollen analyses from a 50000-yr rodent midden series in the southern Atacama desert (25°30′S), *J. Quat. Sci.*, *20*, 493–507.

Marinov, I., A. Gnanadesikan, J. R. Toggweiler, and J. L. Sarmiento (2006), The Southern Ocean biogeochemical divide, *Nature*, *441*, 964–967.

Markgraf, V., J. A. Rodson, P. A. Kershaw, M. S. McGlone, and N. Nicholls (1992), Evolution of the Late Pleistocene and Holocene climates in the circum-South Pacific land areas, *Clim. Dyn.*, *6*, 193–211.

Marti, O., et al. (2005), The new IPSL Climate System Model: IPSL-Cm4, *Note Pole Model.*, *26*, Inst. Pierre-Simon Laplace, Paris.

Martin, J. H. (1990), Glacial-interglacial CO_2 change: The iron hypothesis, *Paleoceanography*, *5*, 1–13.

McElroy, M. B. (1983), Marine biological controls on atmospheric CO_2 and climate, *Nature*, *302*, 328–329.

Menviel, L., A. Timmermann, A. Mouchet, and O. Timm (2008), Meridional reorganizations of marine and terrestrial productivity during Heinrich events, *Paleoceanography*, *23*, PA1203, doi:10.1029/2007PA001445.

Mikaloff Fletcher, S. E., et al. (2006), Inverse estimates of anthropogenic CO_2 uptake, transport, and storage by the ocean, *Global Biogeochem. Cycles*, *20*, GB2002, doi:10.1029/2005GB002530.

Moreno, P. I., T. V. Lowell, G. L. Jacobson Jr., and G. H. Denton (1999), Abrupt vegetation and climate changes during the last glacial maximum and last termination in the Chilean lake district: A case study from Canal de la Puntilla (41°S), *Geogr. Ann., Ser. A*, *81*, 285–311.

Mouchet, A., and L. M. Francois (1996), Sensitivity of a Global Oceanic Carbon Cycle Model to the circulation and to the fate of organic matter: Preliminary results, *Phys. Chem. Earth*, *21*, 511–516.

Omta, A. W., J. Bruggeman, S. A. L. M. Kooijman, and H. A. Dijkstra (2006), Biological carbon pump revisited: Feedback mechanisms between climate and the Redfield ratio, *Geophys. Res. Lett.*, *33*, L14613, doi:10.1029/2006GL026213.

Opsteegh, J. D., R. J. Haarsma, F. M. Selten, and A. Kattenberg (1998), ECBILT: A dynamic alternative to mixed boundary conditions in ocean models, *Tellus, Ser. A*, *50*, 348–367.

Otto-Bliesner, B. L., E. C. Brady, G. Clauzet, R. Tomas, S. Levis, and Z. Kothavala (2006), Last Glacial Maximum and Holocene climate in CCSM3, *J. Clim.*, *19*, 2526–2544.

Peltier, W. R. (2004), Global glacial isostasy and the surface of the ice-age Earth: The ICE-5G (VM2) model and GRACE, *Annu. Rev. Earth Planet Sci.*, *23*, 335–357.

Petit, J. R., et al. (1999), Climate and atmospheric history of the past 420,000 years from the Vostok ice core, Antarctica, *Nature*, *399*, 429–436.

Rojas, M., P. Moreno, M. Kageyama, M. Crucifix, C. Hewitt, A. Abe-Ouchi, R. Ohgaito, E. C. Brady, and P. Hope (2008), The Southern Westerlies during the Last Glacial Maximum in PMIP2 simulations, *Clim. Dyn.*, doi:10.1007/s00382-008-0421-7, in press.

Sabine, C. L., et al. (2004), The oceanic sink of anthropogenic CO_2, *Science*, *305*, 367–371.

Sexton, D. M. H. (2001), The effect of stratospheric ozone depletion on the phase of the Antarctic oscillation, *Geophys. Res. Lett.*, *28*, 3697–3700.

Shulmeister, J., et al. (2004), The Southern Hemisphere westerlies in the Australasian sector over the last glacial cycle: A synthesis, *Quat. Int.*, *118*, 23–53.

Stephens, B. B., and R. F. Keeling (2000), The influence of Antarctic sea ice on glacial-interglacial CO_2 variations, *Nature*, *404*, 171–174.

Stocker, T. F., A. Timmermann, M. Renold, and O. Timm (2007), Effects of salt compensation on the climate model response in simulations of large changes of the Atlantic Meridional Overturning Circulation, *J. Clim.*, *20*, 5912–5928.

Stuut, J.-B. W., and F. Lamy (2004), Climate variability at the southern boundaries of the Namib (southwestern Africa) and Atacama (northern Chile) coastal deserts during the last 120,000 yr, *Quat. Res.*, *62*, 301–309.

Thompson, D. W. J., and S. Solomon (2002), Interpretation of recent Southern Hemisphere climate change, *Science*, *296*, 895–899.

Timm, O., and A. Timmermann (2007), Simulation of the last 21,000 years using accelerated transient boundary conditions, *J. Clim.*, *20*, 4377–4401.

Toggweiler, J. R., J. L. Russell, and S. R. Carson (2006), Midlatitude westerlies, atmospheric CO_2, and climate change during the ice ages, *Paleoceanography*, *21*, PA2005, doi:10.1029/2005PA001154.

Tschumi, T., F. Joos, and P. Parekh (2008), How important are Southern Hemisphere wind changes for low glacial carbon dioxide? A model study, *Paleoceanography*, doi:10.1029/2008PA001592, in press.

Valero-Garcés, B. L., B. Jenny, M. Rondanelli, A. Delgado-Huertas, S. J. Burns, H. Veit, and A. Moreno (2005), Palaeohydrology of Laguna de Tagua Tagua (34°30′S) and moisture fluctuations in Central Chile for the last 46 000 yr, *J. Quat. Sci.*, *20*, 625–641.

Winguth, A. M. E., D. Archer, J.-C. Duplessy, E. Maier-Reimer, and U. Mikolajewicz (1999), Sensitivity of paleonutrient tracer distributions and deep-sea circulation to glacial boundary conditions, *Paleoceanography*, *14*, 304–323.

Zickfeld, K., J. C. Fyfe, M. Eby, and A. J. Weaver (2008), Comment on "Saturation of the Southern Ocean CO_2 sink due to recent climate change,", *Science*, *319*, 570b.

L. Menviel, Department of Oceanography, University of Hawai'i, 1000 Pope Road, Honolulu, HI 96822, USA. (menviel@hawaii.edu)

A. Mouchet, Département AGO, Université de Liège, B-4000 Liège, Belgium.

O. Timm and A. Timmermann, IPRC, SOEST, University of Hawai'i, Honolulu, HI 96822, USA.